Conductive atomic force microscopy investigation of transverse current across metallic and semiconducting single-walled carbon nanotubes

Chiara Baldacchini and Salvatore Cannistraro[a)]
Biophysics and Nanoscience Centre, INFM and CNISM, Facoltà di Scienze, Università della Tuscia, Largo dell'Università, I-01100 Viterbo, Italy

(Received 15 June 2007; accepted 27 August 2007; published online 17 September 2007)

The comprehension of conduction mechanisms in single-walled carbon nanotubes is a crucial task for developing efficient nanodevices. Appealing hybrid architectures could exploit charge transport perpendicular to the main nanotube axis in order to minimize carrier path and phonon scattering effects. Such transverse transport is investigated in metallic and semiconducting nanotubes by means of conductive atomic force microscopy. The transverse current response is interpreted in the framework of a tunneling transport model, and reveals that conduction across metallic nanotubes is either tunneling- or bandlike, depending on the force applied by the tip, while charge carriers always tunnel through the semiconducting nanotubes. © *2007 American Institute of Physics*.
[DOI: 10.1063/1.2785168]

Single-walled carbon nanotubes (SWNTs) are among the most fascinating protagonists in nanoscience at the present days, thanks to their peculiar electronic properties and potential application in nanosized devices.[1] By coupling SWNTs with biomolecules, single biorecognition events can be transduced into electrical signals which, in turn, may be processed by macroscopic circuits.[2] For electronic purposes, SWNTs are mostly studied as lying down on insulating surfaces (contacted by metal electrodes at their ends)[3–5] or standing up on metal surfaces,[6] carrying electrical signals along their main axis. Longitudinal conduction depends on nanotube structure,[7] and it can be tuned in metallic SWNTs by controlling the radial deformation.[5] When SWNTs lie on metal surfaces, current may flow perpendicularly to the main axis. This geometry is suitable for biodevice application, for instance, to connect bioactive sites on the upper nanotube side to underlying metal electrodes.[8] Such a transverse transport is interesting, because carrier path through SWNTs (1–4 nm) is smaller than phonon scattering mean free path (10 nm).[4] Nevertheless, transverse conduction properties of SWNTs are still awaiting a complete characterization.

We studied transverse transport across metallic and semiconducting SWNTs lying on gold surfaces by means of conductive atomic force microscopy (CAFM). CAFM is suitable to study nanostructure electrical properties,[9,10] because it couples morphology and conduction characterization by acquiring simultaneous topographical and current images and *I-V* characteristics. Indeed, the controllable force exerted by the metal-coated tip on the sample allows establishing simultaneous physical and electrical contacts, and current signals can be recorded by applying a bias between tip and substrate.[11] The current response of SWNTs has been previously used to discriminate metallic from semiconducting tubes based on their different longitudinal *I-V* characteristics.[3,5] We observed that also the transverse current response is a fingerprint univocally discriminating metallic from semiconducting SWNTs, and by interpreting the current data in the framework of a tunneling transport model, we highlighted a competition between tunneling- and bandlike mechanisms in transverse conduction across metallic SWNTs.

SWNTs were dispersed on freshly annealed Au(111) surfaces in 1,2-dichloethane solution (1 mg/ml) after 1 h sonication. A detailed Raman spectroscopy investigation was performed (Labram, Jobin-Ivon; 633 nm excitation wavelength). The analysis of radial breathing modes frequency and *G*-band lineshape allowed us to determine the metallic or semiconducting character of individual SWNTs.[12] CAFM measurements (Picoscan, Molecular Imaging Co.) were done at room temperature in pure nitrogen atmosphere with Pt-coated tips (force constant of 0.6 N/m). Topographical CAFM images allow selecting nanotubes with diameter smaller than 3 nm. Current imaging and transverse current data individuate two distinct sets of SWNTs, characterized by (i) well contrasted current images and linearly voltage dependent *I-V* curves at low bias (±0.1 V) and (ii) imaged current features in the range of instrument sensitivity (few pA, up to bias of ±1.0 V) and current response curves with energy gaps at zero bias. By coupling these results with Raman spectroscopy data, SWNTs belonging to the first set are classified as metallic and the others as semiconducting.

Concerning metallic SWNTs, a selected set of transverse current curves are shown in Fig. 1(a). They have been collected at different loading forces across the nanotube whose current image is shown in the inset. At low applied loads, curves are sigmoidal shaped and current intensity increases with the applied force, reaching its maximum at 20.6 nN. Here, the total resistance (as estimated by linearly fitting the curve within ±0.05 V) is $R=4.0\times10^6\ \Omega$. Such a value should be mainly attributed to contact resistances, since the intrinsic resistance of metallic SWNTs is $6.5\times10^4\ \Omega$. Surprisingly, with further increasing the loading force, current drops and curves become sigmoidal again. Such an oscillation is better highlighted by analyzing the transverse conductance (dI/dV). Selected conductance curves are shown in Fig. 1(b): at zero applied voltage, dI/dV presents either a minimum or a maximum, depending on the applied force. A conductance decrement due to an increase of contact resistances at high applied forces appears counterintuitive. More

[a)]Author to whom correspondence should be addressed; electronic mail: cannistr@unitus.it

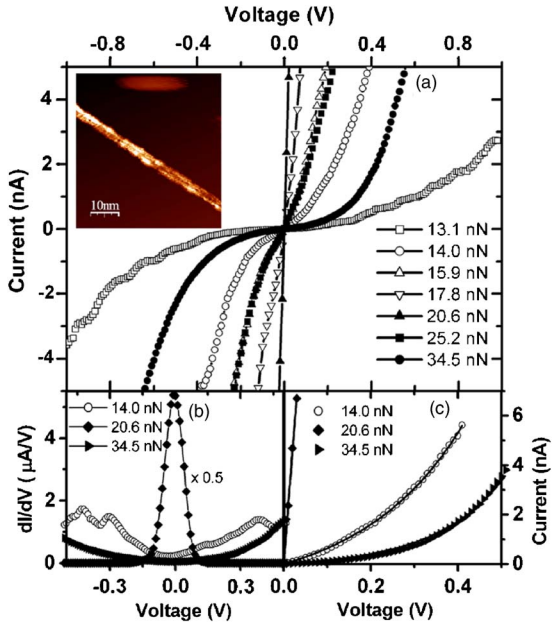

FIG. 1. (Color online) (a) *I-V* curves at different applied forces across a metallic SWNT lying on a gold surface. Inset: current image of the nanotube (at 14.0 nN and bias of 0.5 V, vertical scale: 0.5 nA). (b) Representative *dI/dV* curves. The curve at 34.5 nN is multiplied by 0.5. (c) Best fitting curves (lines) of selected *I-V* characteristics (symbols).

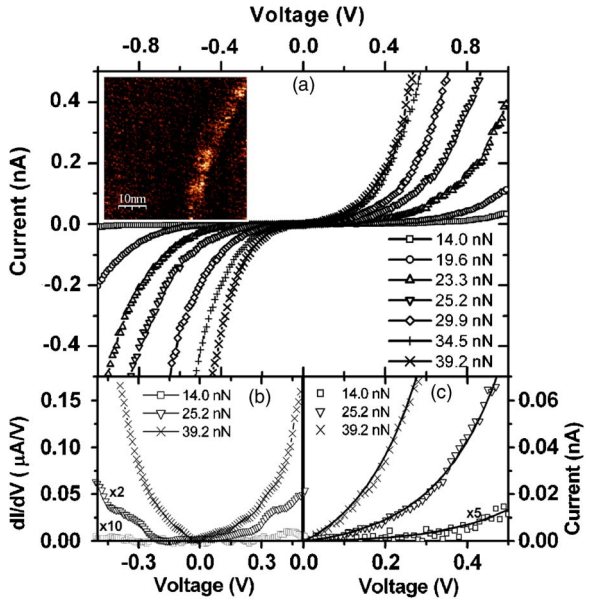

FIG. 2. (Color online) (a) *I-V* curves at different applied forces across a semiconducting SWNT lying on a gold surface. Inset: current image of the nanotube (at 14.0 nN and bias of 0.5 V, vertical scale: 5.0 pA). (b) Representative *dI/dV* curves. Curves at 14.0 nN and 25.2 nN are multiplied by 10 and 2, respectively. (c) Best fitting curves (lines) of selected *I-V* characteristics (symbols). The curve at 14.0 nN is multiplied by 5.

likely, conductance could drop as a result of structural modifications, as previously observed for longitudinal conductance at contact forces higher than 50.0 nN.[5]

For semiconducting nanotubes, at each applied force, *I-V* curves are sigmoidal shaped [Fig. 2(a)], and the conductance has a minimum at zero bias [Fig. 2(b)]. Current and conductance monotonically increase with the loading force, always remaining about two orders of magnitude lower than those measured for metallic SWNTs (vaguely contrasted current images are obtained, inset). *I-V* curves present an energy gap of about 1.3 eV at zero bias, which is constant up to 19.6 nN and decreases at higher loads. The gap probably originates from an energy barrier arising at the nanotube-Au interface,[13] owing to the *n*-type character of semiconducting SWNTs in nitrogen atmosphere.[14] Band gap opening is ruled out, because it is related to the geometrical SWNT structure, and band gaps cannot decrease under mechanical stress.

To clarify transverse conduction mechanisms, *I-V* data have been analyzed in the framework of a transport model including both carrier tunneling (which might occur either through empty space, normal to the nanotube axis, or through bonds on nanotube sidewalls) and bandlike transport. The current is $I=GV$, where $G=G_0T$ is the conductance Landauer formula.[15] G_0 represents the quantum of conductance and T the total transmission probability, given by the product of three terms: $T=T_{\mathrm{Au}}T_{\mathrm{tip}}T_{\mathrm{NT}}$. T_{Au} and T_{tip} refer to SWNT-surface and SWNT-tip interfaces, respectively, and they can be assumed as mainly due to the corresponding contact resistances. T_{NT} describes transport mechanism across the nanotube, and it is given by $e^{-\beta L}$, where L is the tunneling barrier length and β the tunneling decay parameter,[15]

$$\beta = \frac{4\pi}{h}\sqrt{2m^*\alpha\left(H-\frac{\mathrm{eV}}{2}\right)}.$$

Here, h is the Planck constant, m^* is the effective electron mass ($0.16m_e$), H is the barrier height, V is the applied voltage, and α is a parameter describing asymmetric contacts with the electrodes. When bandlike transport occurs, T_{NT} reduces to unity, and the current becomes $I=V/R$, where R is a constant including contact and intrinsic nanotube resistances. Although bandlike transport is not Ohmic in SWNTs,[3] due to electron-phonon scattering,[4] Ohm's law can be used to describe transverse conduction, being carrier path smaller than phonon scattering mean free path.

Current curves recorded across several SWNTs have been fitted through $I=(T_{\mathrm{Au}}T_{\mathrm{tip}})G_0e^{-\beta L}V$. Figures 1(c) and 2(c) show the positive bias regions of representative *I-V* characteristics with their best fitting curves and the corresponding fitting parameters are reported in Tables I and II. The barrier length L, at low applied forces, is consistent with the SWNT diameter, as measured by topographical images. L decreases with increasing the applied force, together with the barrier height H, confirming radial deformation. The asymmetry parameter α is about 1.0 for the semiconducting nanotube (almost equivalent contacts with tip and substrate), while it is about 0.2 for the metallic one, except for high applied loads.

TABLE I. Barrier length L, barrier height H, asymmetry parameter α, and decay constant β as a function of the applied loads, obtained by fitting the *I-V* curves measured across a metallic SWNT.

Force (nN)	L (nm)	H (eV)	α	β (Å^{-1})
13.1	2.90	1.25	0.2	0.20
14.0	3.00	0.50	0.2	0.12
15.9	2.20	0.40	0.2	0.11
17.8	2.20	0.15	0.2	0.06
20.6	0.01	0.05	0.2	0.05
25.2	2.20	0.50	0.2	0.12
34.5	2.10	0.45	0.9	0.26

TABLE II. Barrier length L, barrier height H, asymmetry parameter α, and decay constant β as a function of the applied loads, obtained by fitting the I-V curves measured across a semiconducting nanotube.

Force (nN)	L (nm)	H (eV)	α	β (Å^{-1})
14.0	3.00	0.90	1.0	0.38
19.6	2.90	0.80	1.0	0.36
23.3	2.60	0.75	1.0	0.35
25.2	2.55	0.65	1.0	0.33
29.9	2.60	0.55	1.0	0.30
34.5	2.60	0.45	1.0	0.27
39.2	2.55	0.45	1.0	0.27

To gain further insight into the evolution of transport regime across nanotubes as a function of the applied force, we analyzed the tunneling decay parameter β (calculated at $V=0$ [Fig. 3(a)]), because it reflects the medium capability to sustain the tunneling charge transport. For semiconducting nanotubes, at low contact forces, β is about 0.35–0.40 Å^{-1} consistently with tunneling transport through π-conjugated molecules.[15] β monotonically decreases with incrementing the applied force, due to the tunneling barrier reduction under mechanical compression. This confirms that the gap observed in the I-V curves could originate from tunneling effects rather than from band gap opening. For metallic SWNTs, β is about 0.20 Å^{-1} at very low applied forces, and it rapidly cancels out as soon as the contact force increases. When β is about 0 (at 20.6 nN), T_{NT} reduces to 1; therefore, the tunneling contribution becomes negligible, and the transport switches to bandlike. With further raising the applied load, β reverts to be significant, reaching the value characteristic of the semiconducting nanotubes under comparable mechanical stress (0.26 Å^{-1}), and the conduction returns tunnelinglike. The total resistance R across the metallic SWNT is shown in Fig. 3(b). Beside contact and intrinsic resistances, R could include tunneling resistances, which may depend on tunneling barrier length and on the medium sustaining charge tunneling.[16] Indeed, R logarithmically has the same trend of β, with increasing the applied force: it initially decreases, due to the lowering of the barrier length, and then increases, likely due to the modification of the SWNT structure.

Finally, the evolution of β and α in metallic SWNTs suggests that tunneling like transport regimes observed at low and high applied forces might have different origins. At low loading forces, the nanotube structure and its metallic character (probably playing a role in the conduction, as suggested by the inconsistently low α value) are preserved, and charge carriers tunneling may be due to high resistance contacts, as for longitudinal transport.[5] On the contrary, at high applied forces, metallic SWNTs show conduction characteristics reminiscent of those of semiconducting ones, accordingly to the formation of a barrier, as due to a mechanically induced symmetry breaking.

In conclusion, by means of CAFM, we deeply characterized the transverse current response across SWNTs, which is interesting for application in bioelectronics, also because the carrier path could be lower than phonon scattering mean free path. Through the transverse current response, CAFM is able to single out semiconducting and metallic SWNTs by locally applying forces lower than 30 nN and biases within ± 1.0 V. The transverse transport mechanism is elucidated in the framework of a tunneling transport model: charge carriers tunnel across semiconducting nanotubes, while transport regime switches between tunneling- and bandlike across metallic SWNTs as a function of the loading force.

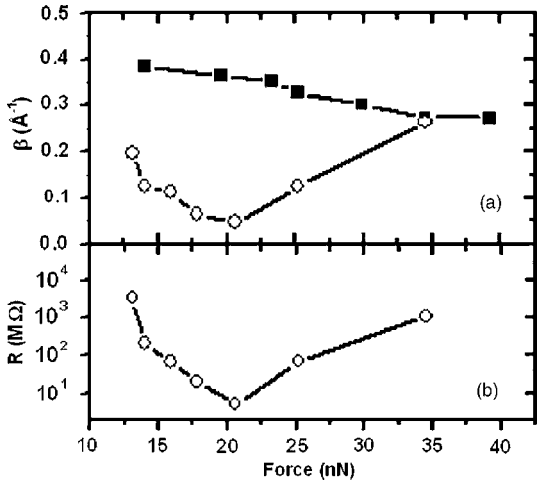

FIG. 3. (a) Tunneling decay parameter β as a function of the applied force for a metallic (open symbols) and a semiconducting (closed symbols) SWNT lying on a gold surface. (b) Total resistance R across the metallic SWNT, as derived by linearly fitting the I-V curves between ±0.05 V.

Work partially supported by the PRIN-MIUR Research Project (Grant No. 2006028219). Authors are grateful to Dr. Laura Andolfi for experimental support.

[1] H. Dai, Surf. Sci. **500**, 218 (2002).
[2] G. Gruner, Anal. Bioanal. Chem. **384**, 322 (2006).
[3] P. J. de Pablo, C. Gómez-Navarro, J. Colchero, P. A. Serena, J. Gómez-Herrero, and A. M. Baró, Phys. Rev. Lett. **88**, 036804 (2002).
[4] A. Javey, J. Guo, M. Paulsson, Q. Wang, D. Mann, M. Lundstrom, and H. Dai, Phys. Rev. Lett. **92**, 106804 (2004).
[5] C. Gómez-Navarro, J. J. Sáenz, and J. Gómez-Herrero, Phys. Rev. Lett. **96**, 076803 (2006).
[6] F. Patolsky, Y. Weizmann, and I. Willner, Angew. Chem., Int. Ed. **43**, 2113 (2004).
[7] T. W. Tombler, C. Zhou, L. Alexseyev, J. Kong, H. Dai, L. Liu, C. S. Jayanthi, M. Tang, and S.-Y. Wu, Nature (London) **405**, 769 (2000).
[8] I. Delfino, B. Bonanni, L. Andolfi, C. Baldacchini, A. R. Bizzarri, and S. Cannistraro, J. Phys.: Condens. Matter **19**, 225009 (2007).
[9] E. Nahym, Y. Ebenstein, A. Aharoni, T. Mokari, U. Banin, N. Shimoni, and O. Millo, Nano Lett. **4**, 103 (2003).
[10] L. Andolfi and S. Cannistraro, Surf. Sci. **598**, 68 (2005).
[11] L. Andolfi, A. R. Bizzarri, and S. Cannistraro, Appl. Phys. Lett. **89**, 183125 (2006).
[12] M. S. Dresselhaus, G. Dresselhaus, A. Jorio, A. G. Souza Filho, and R. Saito, Carbon **40**, 2043 (2002).
[13] Y. Yaish, J.-Y. Park, S. Rosenblatt, V. Sazonova, M. Brink, and P. L. McEuen, Phys. Rev. Lett. **92**, 046401 (2004).
[14] X. Cui, M. Freitag, R. Martel, L. Brus, and P. Avouris, Nano Lett. **3**, 783 (2003).
[15] A. Salomon, D. Cahen, S. Lindsay, J. Tomfohr, V. B. Engelkes, and C. D. Frisbie, Adv. Mater. (Weinheim, Ger.) **15**, 1881 (2003).
[16] D. Alliata, L. Andolfi, and S. Cannistraro, Ultramicroscopy **101**, 231 (2004).